OPEN

Morphologic and Molecular Heterogeneity of High-grade Serous Carcinoma Precursor Lesions

Yen-Wei Chien, MD,† Yeh Wang, MD, PhD,‡ Peng Huang, PhD,§‖ Barrett Craig Lawson, MD,¶ David L. Kolin, MD,# M. Herman Chui, MD,** Russell Vang, MD,‡ Tricia A. Numan, MD,‡ T. Rinda Soong, MD,†† Brant G. Wang, MD,‡‡§§‖‖ Saron Ann Smith, MD,¶¶ Chi-Long Chen, MD, PhD,## Rebecca Stone, MD,* Christopher Douville, PhD,§ Tian-Li Wang, PhD,*‡ and Ie-Ming Shih, MD, PhD*‡*

Downloaded from http://journals.lww.com/ajsp by BhDMf5ePHKav1zEoum1tQfN4a+kJLhEZgbsIHo4XMi0hCywCX1AWnYQp/IlQrHD3i3D0OdRyi7TvSFl4Cf3VC4/OAVpDDa8K2+Ya6H515kE= on 09/11/2024

Abstract: Serous tubal intraepithelial carcinoma (STIC) is the fallopian tube precursor lesion for most cases of pelvic high-grade serous carcinoma (HGSC). To date, the morphologic, molecular, and clinical heterogeneity of STIC and a less atypical putative precursor lesion, termed serous tubal intraepithelial lesion, has not been well characterized. Better understanding of precursor heterogeneity could impact the clinical management of women with incidental STICs (without concurrent carcinoma) identified in cases of prophylactic or opportunistic salpingectomy. This study analyzed morphologic and molecular features of 171 STICs and 21 serous tubal intraepithelial lesions. We assessed their histologic features, Ki-67 and p53 staining patterns, and genome-wide DNA copy number alterations. We classified all precursor lesions into 2 morphologic subtypes, one with a flat surface (Flat) and the other characterized by budding, loosely adherent, or detached (BLAD) morphology. On the basis of pathology review by a panel of 8 gynecologic pathologists, we found 87 BLAD, 96 Flat, and 9 indeterminate lesions. As compared with Flat lesions, BLAD lesions were more frequently diagnostic of STIC ($P < 0.0001$) and were found concurrently with HGSC ($P < 0.0001$). BLAD morphology was also characterized by higher Ki-67 proliferation index ($P < 0.0001$), presence of epithelial stratification ($P < 0.0001$), and increased lymphocyte density ($P < 0.0001$). BLAD lesions also exhibited more frequent DNA copy number gain/amplification at the *CCNE1* or *CMYC* loci canonical to HGSCs ($P < 0.0001$). Both BLAD morphology and STIC diagnoses are independent risk factors for an elevated Ki-67 proliferation index. No correlation was observed between BLAD and Flat lesions with respect to patient age, presence of germline *BRCA1/2* mutation, or p53 staining pattern. These findings suggest that tubal precursor lesions are morphologically and molecularly heterogeneous, laying the foundation for further studies on the pathogenesis of HGSC initiation and identifying histologic features predictive of poor patient outcomes.

Key Words: ovarian cancer, STIC, aneuploidy, risk stratification

(*Am J Surg Pathol* 2024;48:475–486)

From the *Departments of Gynecology and Obstetrics; ‡Pathology, Johns Hopkins Medical Institutions; §Department of Oncology, Division of Quantitative Science, The Sidney Kimmel Comprehensive Cancer Center at Johns Hopkins, Johns Hopkins University School of Medicine; ‖Department of Biostatistics, Johns Hopkins Bloomberg School of Public Health, Baltimore, MD; ¶Department of Pathology, MD Anderson Cancer Center, Houston, TX; #Department of Pathology, Brigham and Women's Hospital, Boston, MA; **Department of Pathology and Laboratory Medicine, Memorial Sloan Kettering Cancer Center, New York, NY; ††Department of Pathology, University of Pittsburgh School of Medicine, Pittsburgh, PA; ‡‡Department of Pathology, Inova Fairfax Hospital; §§University of Virginia School of Medicine Inova Campus, Falls Church, VA; ‖‖Department of Pathology, Georgetown University Medical Center, Washington, DC; ¶¶Legacy Health Systems, Portland, OR; †Department of Pathology, Taipei Municipal Wan-Fang Hospital, Taipei Medical University; and ##Department of Pathology, Taipei Medical University, Taipei, Taiwan.

Supported by the Break Through Cancer (BTC-IOC), the Richard W. TeLinde Endowment from the Johns Hopkins University, NIH/NCI (U2CCA271891, P50CA228991, R01CA260628, and R01CA215483). C.D. is a consultant to Exact Sciences and has been paid in equity and income. C.D. is a founder of Belay Diagnostics. C.D. is an inventor of some technologies. The companies named above as well as other companies have licensed previously described technologies related to the work described in this paper from Johns Hopkins University. Licenses to these technologies are or will be associated with equity or royalty payments to the inventors as well as Johns Hopkins University. The terms of all of these arrangements are being managed by Johns Hopkins University in accordance with its conflict of interest policies.

Conflicts of Interest and Source of Funding: The authors have disclosed that they have no significant relationships with, or financial interest in, any commercial companies pertaining to this article.

Correspondence: Ie-Ming Shih, MD, PhD, Departments of Gynecology and Obstetrics, Pathology and Oncology, Johns Hopkins Medical Institutions, 1550 Orleans Street, Rm 305 Baltimore 21231, MD (e-mail: ishih@jhmi.edu).

Supplemental Digital Content is available for this article. Direct URL citations are provided in the HTML and PDF versions of this article on the journal's website, www.ajsp.com.

Copyright © 2024 The Author(s). Published by Wolters Kluwer Health, Inc. This is an open access article distributed under the terms of the Creative Commons Attribution-Non Commercial-No Derivatives License 4.0 (CCBY-NC-ND), where it is permissible to download and share the work provided it is properly cited. The work cannot be changed in any way or used commercially without permission from the journal.

High-grade serous carcinoma (HGSC), the most common histologic type of ovarian cancer in western countries, is unique among human neoplastic diseases because it is unlikely to originate from its cognate tissue, the ovary, which is covered by a thin layer of

Downloaded from http://journals.lww.com/ajsp by BhDMf5ePHKav1zEoum1tQfN4a+kJLhEZgbsIHo4XMi0hCywCX1AWnYQp/IlQrHD3i3D0OdRyi7TvSFl4Cf3VC4/OAVpDDa8K2+Ya6H515kE= on 09/11/2024

mesothelium.[1] Although HGSC has traditionally been considered to emerge from the ovarian surface, direct evidence of mesothelial precancerous lesions on the ovarian surface preceding HGSC is largely lacking. About 2 decades ago, a new paradigm proposed that most HGSCs originate from fallopian epithelium, from a precursor termed serous tubal intraepithelial carcinoma (STIC).[2,3] This paradigm has been supported by a wealth of clinicopathological and molecular studies.[1,4–9]

STICs are of microscopic size and are detected on the mucosal surface of the fallopian tube, commonly at the fimbriated ends. Classic morphologic features of STICs include nuclear atypia, prominent nucleoli, epithelial stratification, and occasional mitotic figures and/or apoptotic bodies.[10–12] STICs can be found with or without concurrent HGSC, and isolated STICs detected incidentally, in the absence of HGSC, arguably provide the ideal tissue sources for studying the pathogenesis of HGSC. Alongside STIC that may represent the immediate precursor of many HGSCs, other related lesions have been recognized. Among these tubal lesions, serous tubal intraepithelial lesion (STIL) is defined by the presence of cellular and architectural atypia, which is not as severe as STICs. Immunostaining is helpful to distinguish STIC from STIL. Although there is no universal consensus, a Ki-67 index has been proposed as one of the diagnostic criteria to distinguish STIC from STIL, and some researchers consider STIL to be a form of proliferatively dormant STIC.[13] STICs have a higher Ki-67 labeling index, and a cutoff value of 10% has been used to distinguish STIC from STIL.[10,14–16] Both STICs and STILs harbor *TP53* missense or truncating mutations.[4,5] The combination of morphologic features and immunostaining using p53 and Ki-67 antibodies is the current standard of practice used by pathologists to make the diagnosis of STIC and STIL.[15] The group of tubal lesions without morphologic atypia but showing a p53-missense–type immunostaining pattern are termed p53 signature. In clinical practice, p53 signatures cannot be identified on a basis of routine hematoxylin and eosin staining unless p53 immunohistochemistry is applied.[17]

Recent studies have shed light on the molecular landscape of STIC and STIL, revealing key molecular alterations involved in their development.[1,13,18–20] However, the heterogeneity of tubal precursor lesions has not been well characterized. With the increasing adoption of opportunistic salpingectomy as a preventive measure for HGSC in average-risk women,[21,22] in addition to prophylactic salpingo-oophorectomy in the high-risk population, pathologists are likely to encounter an increasing number of tubal precursor lesions in routine surgical pathology practice. STICs are clinically significant due to their potential association with HGSC after salpingectomy.[9,23,24] However, one of the most important unanswered questions is whether certain morphologic and/or molecular features of STICs are associated with the risk of subsequent malignancy. At present, it is debatable whether incidental STIC diagnosis should prompt further clinical action to prevent the development of invasive HGSC since there is no published guideline. A recent analysis showed that nearly 30% of *BRCA* mutation carriers found to have STIC at the time of risk-reducing bilateral salpingo-oophorectomy will develop HGSC within 10 years.[9,23,24] This suggests that not all STICs are the same, with some being more clinically aggressive than others. To understand which STIC portends a poor prognosis and warrants further intervention, we characterized the morphologic and molecular diversity among different types of tubal precursor lesions.

This study aims to establish a morphologic marker, and it shows that tubal precursor lesions can be dichotomized into 2 major morphologic subtypes with high reproducibility: flat surface (Flat) and Budding, Loosely Adherent, or Detached (BLAD) morphologies that distinctly differ in Ki-67 proliferation index, degree of epithelial stratification, lymphocyte density, and DNA copy number alteration patterns. These findings provide a foundation for future research on the risk stratification of tubal precursor lesions and the study of ovarian cancer pathogenesis.

MATERIALS AND METHODS

Tissue Acquisition

Cases with a diagnosis of STIC or STIL were identified in the pathology archives at the Johns Hopkins Medical Institutions in Baltimore, MD, and the Inova Fairfax Hospital in Fairfax, VA. The diagnoses of those lesions were finalized in consensus pathology meetings at the local hospitals using the criteria defined in a previous study.[17] Formalin-fixed and paraffin-embedded tissue blocks as well as the original hematoxylin and eosin staining slides were obtained. This study was conducted in accordance with ethical guidelines (eg, Declaration of Helsinki, CIOMS, Belmont Report, US Common Rule) and with the approval of the local institutional review boards. Informed consent was waived. We identified a total of 192 tubal lesions from 124 women. We used laser capture-microdissection to enrich the epithelial cells. Genomic DNA from individual specimen was extracted using the QIAmp formalin-fixed and paraffin-embedded DNA tissue kit (Qiagen, 56404), as previously reported.[5,25]

Histologic Review of Morphologic Features

Whole hematoxylin and eosin staining slides were scanned using the NanoZoomer S60 Digital slide scanner, and the individual STICs and STILs were manually annotated. The image files were uploaded and shared among all investigators in this study through the Concentriq Proscia pathology platform. The images in this study are available upon request to the corresponding author. A panel of 8 gynecologic pathologists (Y.C., M.H.C., D.K., B.C.L., R.S.V., T.N., T.R.S., and I.M.S.) from 5 institutions participated in the review of the following histologic characteristics of cases: (1) presence of signs of discohesiveness, (2) presence of epithelial stratification (single layer vs. multiple layers of lesion cells), and (3) intraepithelial and subepithelial/stromal density of lymphocytes (increased vs. not increased).

Copyright © 2024 The Author(s). Published by Wolters Kluwer Health, Inc.

Downloaded from http://journals.lww.com/ajsp by BhDMf5ePHKav1zEoum1tQfN4a+kJLhEZgbsIHo4XMi0hCywCX1AWnYQp/IlQrHD3i3D0OdRyi7TvSFl4Cf3VC4/OAVpDDa8K2+Ya6H515kE= on 09/11/2024

On the basis of initial assessment, we created 3 morphologic groups of tubal lesions (BLAD, Flat, and indeterminate). BLAD lesions were defined by budding and loosely adherent and detached single cells or small clusters of lesion cells in more than 10 percent of the evaluable area. Flat lesions lacked these features and exhibited relatively flat and intact surfaces in >90% of the lesion. Epithelial stratification was categorized as single, multiple, or indeterminate. Lymphocyte density inside the epithelium and the stroma underneath a lesion (at a depth of ~100 to 200 μm) was classified as increased, not increased, or indeterminate. This was based on comparing the lesion to the adjacent histologically unremarkable tubal epithelium. We used a democratic system to assign a lesion to the BLAD, Flat, or indeterminate group based on a majority vote rule. In addition, if equal numbers of votes were received for more than 1 category, the lesion was also classified as "indeterminate." The same approach was applied to the epithelial stratification and to lymphocyte density.

Immunohistochemistry

Immunohistochemical analysis of p53 and Ki-67 was performed in all cases either at the time of clinical diagnosis or at the time of this study. Immunostaining was performed using an anti-p53 mouse monoclonal antibody (Roche, 760-2542. Bp53-11 clone) and an anti-Ki-67 antibody (Roche, 790-4286, 30-9 clone). Among the 192 lesions studied, 105 p53-immunostained slides and 125 Ki-67-immunostained slides were accessible for interpretation. Interpretation of p53 staining followed the previously reported criteria. Briefly, an intense and diffuse nuclear immunoreactivity suggested a missense *TP53* mutation; complete negativity a mutation causing loss of p53 protein expression; focal and weak staining a wild-type *TP53* status. Diffuse staining is defined as expression in >60% of epithelial cells.[26] We only considered nuclear p53 staining in this study despite cytoplasmic staining may have biological significance. To estimate the Ki-67 labeling index, at least 100 cells were counted, if available. A normalized Ki-67 index was calculated as the ratio of the Ki-67 index of the lesion to the Ki-67 index of the histologically unremarkable tubal epithelial cells on the same sections.

Assessment of Aneuploidy Using the Repetitive Element Aneuploidy Sequencing System

To determine genome-wide DNA copy number alterations, we used Repetitive Element AneupLoidy Sequencing System (RealSeqS), which was previously detailed.[27] We have recently applied this technique in the analysis of aneuploidy patterns in cfDNA and cytologic specimens from esophagus.[28] Briefly, we PCR-amplified ~350,000 repetitive sites across the human genome. Each sample was analyzed in 8 separate assays, with 100 to 250 pg of DNA in each reaction. We conducted a second PCR round to incorporate barcodes into each PCR product. Before sequencing, we purified amplification products from the second cycle using the AMPure XP beads (Beckman cat # a63880) in accordance with the manufacturer's instructions.

The assessment of aneuploidy in terms of chromosomal locations and the levels of gain/loss have been described.[27,28] Briefly, we used a pre-existing set of 30 genomic DNA samples from healthy people as normal references. A smaller subset (n = 7) of the reference samples that were most comparable to the amplicon distributions produced by RealSeqS were then matched to each experimental sample. Following that, the statistical significance for the 39 nonacrocentric chromosomal arms was determined.

$$Z_{chr} = \frac{Observed_{chr} - \mu_{chrpanel}}{\sigma_{chrpanel}}$$

If $|Z_{chr}| > 5$, an arm was called aneuploid. More specifically, gain was rendered if $Z_{chr} > 5$ and lost if $Z_{chr} < -5$. The circular binary algorithm (CBS) was applied to generate statistical significances at the arm level for 50 kb nonoverlapping genomic intervals for each experimental sample. The subchromosomal focal changes were recognized by the CBS algorithm. If the CBS produced a subchromosomal segment encompassing the region of interest and had a log2 ratio >0.25, the focal amplification for 19q12, 19q13.2, or 8q24 was declared. Subsequently, using the information from the discovery set, we developed an algorithm to molecularly group STIC, p53 signature, and normal fallopian tube epithelium into several clusters. These patterns of aneuploidy were grouped under the terms of Path 2, Path 3, Path 4, and Path 5 in this study.[29] In this study, we focused on *CCNE1* and *MYC* copy number gain since they are well-known HGSC genes.

Statistical Analysis

Agreement among the 8 pathologists' image readings was assessed by Krippendorff alpha, which is a measure of inter-rater agreement that quantifies the level of agreement among multiple observers. Krippendorff alpha takes values between −1 and 1. A value of −1 indicates perfect disagreement among the raters, 0 indicates an agreement expected by chance, and 1 indicates perfect agreement among the raters. CI of Krippendorff alpha values were obtained through 1000 bootstrap simulations.

The final classification of lesions, based on the majority vote from the readings of 8 pathologists, was used for statistical analyses. The "indeterminate" group was treated as missing data in the analyses. Univariate analysis evaluated associations between morphologic subtype (BLAD vs. Flat) and patient age, germline BRCA status, lesion location (fimbria vs. lumen), epithelial stratification, immunostaining markers (Ki-67 labeling index and p53 staining pattern), and aneuploidy class (Path 2, Path 3, Path 4, and Path 5). Categorical variables were analyzed using Fisher exact test, while continuous variables were assessed using the Wilcoxon rank-sum test. One-way analysis of variance was used to investigate the association between aneuploidy classes and $\log_2$-transformed Ki-67.

Copyright © 2024 The Author(s). Published by Wolters Kluwer Health, Inc.

Downloaded from http://journals.lww.com/ajsp by BhDMf5ePHKav1zEoum1tQfN4a+kJLhEZgbsIHo4XMi0hCywCX1AWnYQp/IlQrHD3i3D0OdRyi7TvSFl4Cf3VC4/OAVpDDa8K2+Ya6H515kE= on 09/11/2024

We repeated this analysis in the subgroup of cases without a diagnosis of HGSC (ie, the incidental lesions). Fisher exact test was used to study the association between categorical variables.

In multivariate analysis, a linear regression model was used to determine whether BLAD and multilayer epithelial stratification were independently associated with elevated Ki-67 after adjusting for STIC versus STIL diagnosis. Log_2 transformation was applied to the Ki-67 index to reduce its skewness. We used a regression tree to explore synergies and interactions among all variables to identify subgroups with varying levels of Ki-67 index. The same analyses were repeated for the BLAD and Flat lesions without concurrent HGSC (ie, the incidental lesions).

RESULTS

Clinicopathologic Features of "Ovarian" Precancerous Lesions

Tubal precursor lesions were retrieved by digitally searching pre-existing pathology reports for diagnoses of STIC and STIL. The diagnoses were reviewed and finalized by at least 2 pathologists who applied the previously reported morphologic and immunohistochemistry-based diagnosis criteria for STIC, STIL, and p53 signature. Despite the terminology in describing tubal lesions has not been standardized other than STIC in clinical practice, this current study included the term, STIL or p53 signature, following the criteria we previously established. STIL is the lesion with nuclear atypia but to a lesser degree as compared with STIC and with Ki-67 proliferation index <10%. p53 signature represents a stretch of tubal epithelial cells showing a p53-missense–type immunostaining pattern but without any recognizable atypia.[17] The study design is schematically summarized in Figure 1A. The clinicopathologic and molecular features of all lesions in this study are listed in Supplementary Table 1, Supplemental Digital Content 1, http://links.lww.com/PAS/B761.

A total of 192 tubal STIC and STIL lesions were analyzed. Within this cohort, 171 (89%) were classified as STIC and 21 (11%) as STIL. Among the 171 STICs, 54 (32%) were incidental (no concurrent HGSC), and among the 21 STILs, 20 (95%) were incidental (Fig. 1B). Photomicrographs of representative STICs and STILs in this study are shown in Figure 2.

To characterize the morphologic heterogeneity among the tubal precursor lesions, we identified histologic patterns that separated the lesions into 2 groups plus a small group of indeterminate lesions. BLAD lesions were characterized by the presence of single or small clusters of STIC or STIL cells showing budding, loose adherence, or detachment from the surface on the 2-D sections. Flat lesions exhibited a smooth and intact surface without any of the BLAD features. Representative BLAD and Flat tubal precursor lesions are shown in Figure 3. On the basis of majority vote from the 8 gynecologic pathologists, we classified the 192 tubal precursor lesions into the following morphologic subtypes: 87 (45%) BLAD lesions, 96 (50%) Flat lesions, and 9 (5%) indeterminate lesions (Fig. 4A). BLAD morphology was highly associated with, and exclusively seen in STIC lesions, whereas the Flat lesions comprised 75 STICs and all 21 STILs ($P < 0.0001$) (Fig. 4B). The 9 lesions in the indeterminate category were all STICs. Regarding the classification into BLAD or Flat groups, there was unanimous agreement for 50% of cases (n = 96) and high agreement (7 of 8 pathologists agreed) for 21% of cases (n = 40). We observed that 64 (36%) lesions had a single epithelial layer, while 113 (64%) lesions had multiple epithelial layers. The remaining 6 lesions were indeterminate. As for epithelial and stromal lymphocyte density, 26 (14%) lesions exhibited increased density, 154 (86%) lesions had a background density, and 3 lesions were indeterminate. For the morphologic categorization as BLAD, Flat, and indeterminate, the Krippendorff alpha value was 0.61 (95% CI: 0.55-0.66), indicating substantial agreement among the 8 pathologists from different institutions.

Features Associated With the BLAD and Flat Lesions

We examined associations between BLAD and Flat morphologies and several clinicopathologic features, including patient age, presence of concurrent HGSC, lesion location, local lymphocyte density, and pattern of p53 staining. BLAD morphology was significantly associated with the presence of concurrent HGSC ($P < 0.0001$) (Fig. 5A; Table 1). We observed that 75 of 87 BLAD lesions (86.2%) had multilayer epithelial stratification, while only 38 of 96 (40%) Flat lesions exhibited this feature ($P < 0.0001$). To identify the best predictor of lesions associated with concurrent HGSCs, we found that among the BLAD lesions and in patients aged > 57, 79.7% (51/64) had concurrent HGSC compared with 52.0% (66/127) in the other group composed of all Flat lesions and BLAD lesions in patients aged ≤ 57 ($P = 0.0003$). Details of these data are provided in Supplementary Table 2, Supplemental Digital Content 2, http://links.lww.com/PAS/B762.

In the entire cohort, we detected increased lymphocyte density in only 26 lesions, as compared with their respective background mucosae, which was associated with BLAD morphology (22/87,25%, vs. 4/ 96, 4% Flat lesions, $P < 0.0001$) (Fig. 5B). This association was also observed within the subgroup of incidental tubal precursor lesions (BLAD, n = 21, Flat, n = 51), in which 24% of BLAD lesions harbored increased lymphocyte density compared with 2% of Flat lesions (2%) ($P = 0.0058$). Photomicrographs of representative lesions with increased lymphocyte density are shown in Figure 5C. Other features, including patient age, *BRCA* germline mutation status, location (fimbria versus ampulla), and p53 staining pattern, did not significantly differ by BLAD and Flat morphologies (all $P > 0.05$).

To further investigate the factors independently associated with BLAD versus Flat morphology, a multivariate analysis was performed. The factors studied in this multivariate analysis included patient age, *BRCA* germline mutation, concurrent HGSC, STIC versus STIL diagnosis,

Copyright © 2024 The Author(s). Published by Wolters Kluwer Health, Inc.

Downloaded from http://journals.lww.com/ajsp by BhDMf5ePHKav1zEoum1tQfN4a+kJLhEZgbsIHo4XMi0hCywCX1AWnYQp/IlQrHD3i3D0OdRyi7TvSFl4Cf3VC4/OAVpDDa8K2+Ya6H515kE= on 09/11/2024

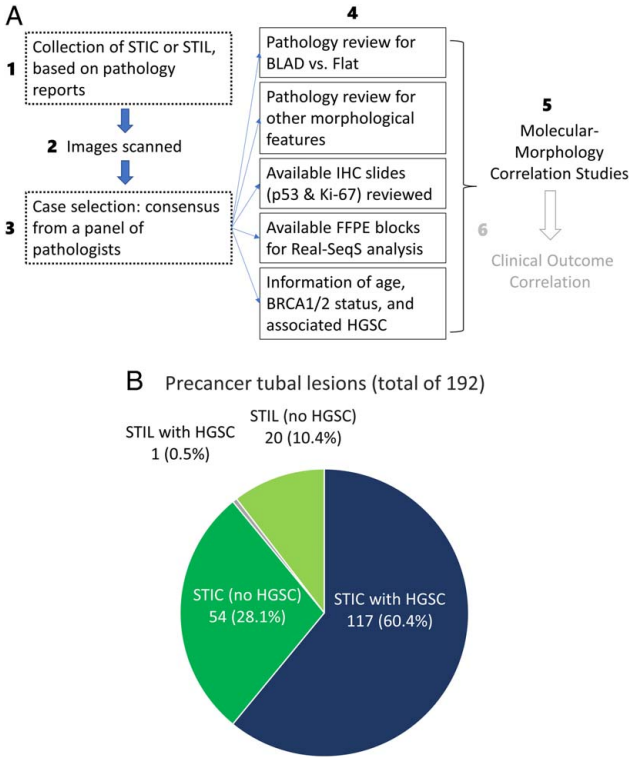

FIGURE 1. Study design and case selection. A, Flowchart schematically showing sequential case selection, pathologic review, and data analysis. B, Diagnosis of the tubal precursor lesions selected in the cohort.

normalized Ki-67 index, epithelial stratification (single layer versus multilayer) and lymphocyte density. After excluding indeterminate lesions and those with missing Ki-67 measures, 163 lesions were included in the multivariate analysis.

Our analysis showed that Ki-67 index, multilayered epithelium, and increased lymphocyte density were independently associated with the BLAD morphology, while *BRCA* germline status, HGSC diagnosis, and STIC diagnosis were not. The association between BLAD morphology and the combination of Ki-67 expression and epithelial stratification was examined, and a cutoff value of normalized Ki-67 index (ratio of 5.67) was found. A group of lesions exhibiting a normalized Ki-67 index ≥ 5.67 and multilayer epithelial stratification were most likely to be associated with BLAD morphology (Table 2).

Comparison of the Proliferative Activity and Aneuploidy Between BLAD and Flat Lesions

The normalized Ki-67 index of BLAD lesions (21.3 ± 20.1) was higher than that in Flat lesions (6.5 ± 8.7) ($P < 0.0001$) (Fig. 6A, left). We found a similar result in a subset analysis of incidental tubal precursor lesions only (no concurrent HGSC). Ki-67 index was significantly elevated in incidental BLAD lesions ($24.1 \pm 19.5\%$) in comparison to incidental Flat lesions ($4.4 \pm 4.5\%$) ($P < 0.0001$) (Fig. 6A, right). Among the 192 lesions, we were able to find tissue blocks still containing the lesions and retrieve a sufficient amount of DNA from 76 lesions for RealSeqS assays to assess amplification/gain in chromosomal regions harboring the *CCNE1* and *MYC* loci. We focus on these genes because they are among the most commonly amplified genes in HGSCs. Among the 76 lesions, the data from 53 lesions were retrieved from our recent study.[29] Using this assay, we found that *CCNE1* and *MYC* gain corresponded to Path 2 and Path 3 aneuploidy patterns in the RealSeqS algorithm, respectively; therefore, we focused

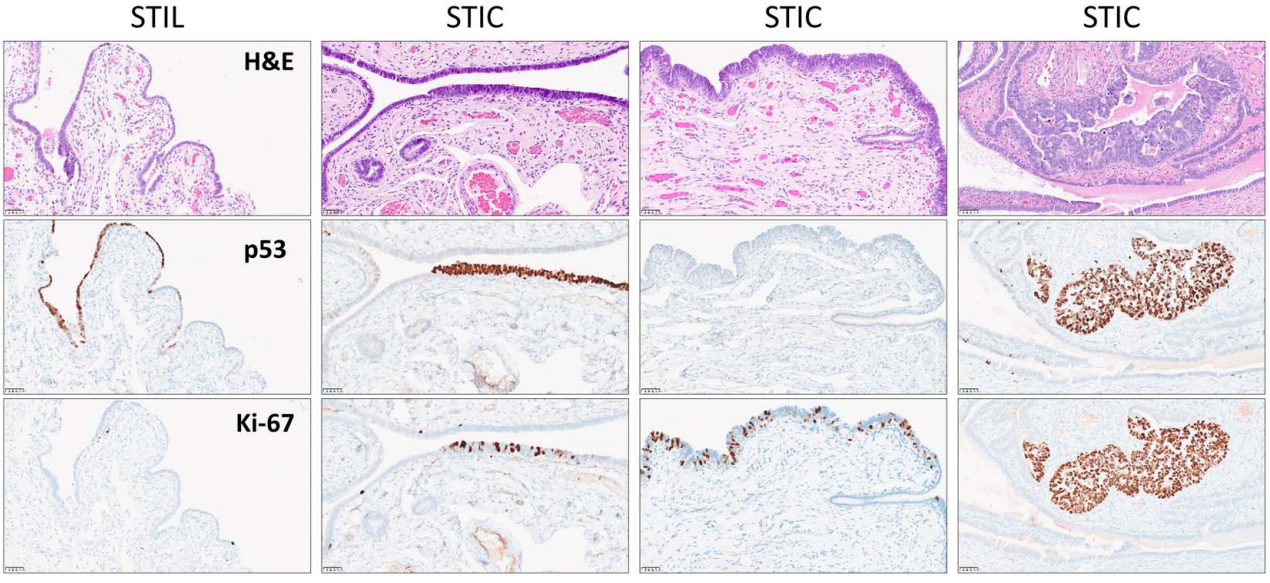

FIGURE 2. Representative photomicrographs of STICs and STILs. H&E (first row), p53 staining (second row), and Ki-67 staining (third row). H&E indicates hematoxylin and eosin staining.

Copyright © 2024 The Author(s). Published by Wolters Kluwer Health, Inc.

Downloaded from http://journals.lww.com/ajsp by BhDMf5ePHKav1zEoum1tQfN4a+kJLhEZgbsIHo4XMi0hCywCX1AWnYQp/IlQrHD3i3D0OdRyi7TvSFl4Cf3VC4/OAVpDDa8K2+Ya6H515kE= on 09/11/2024

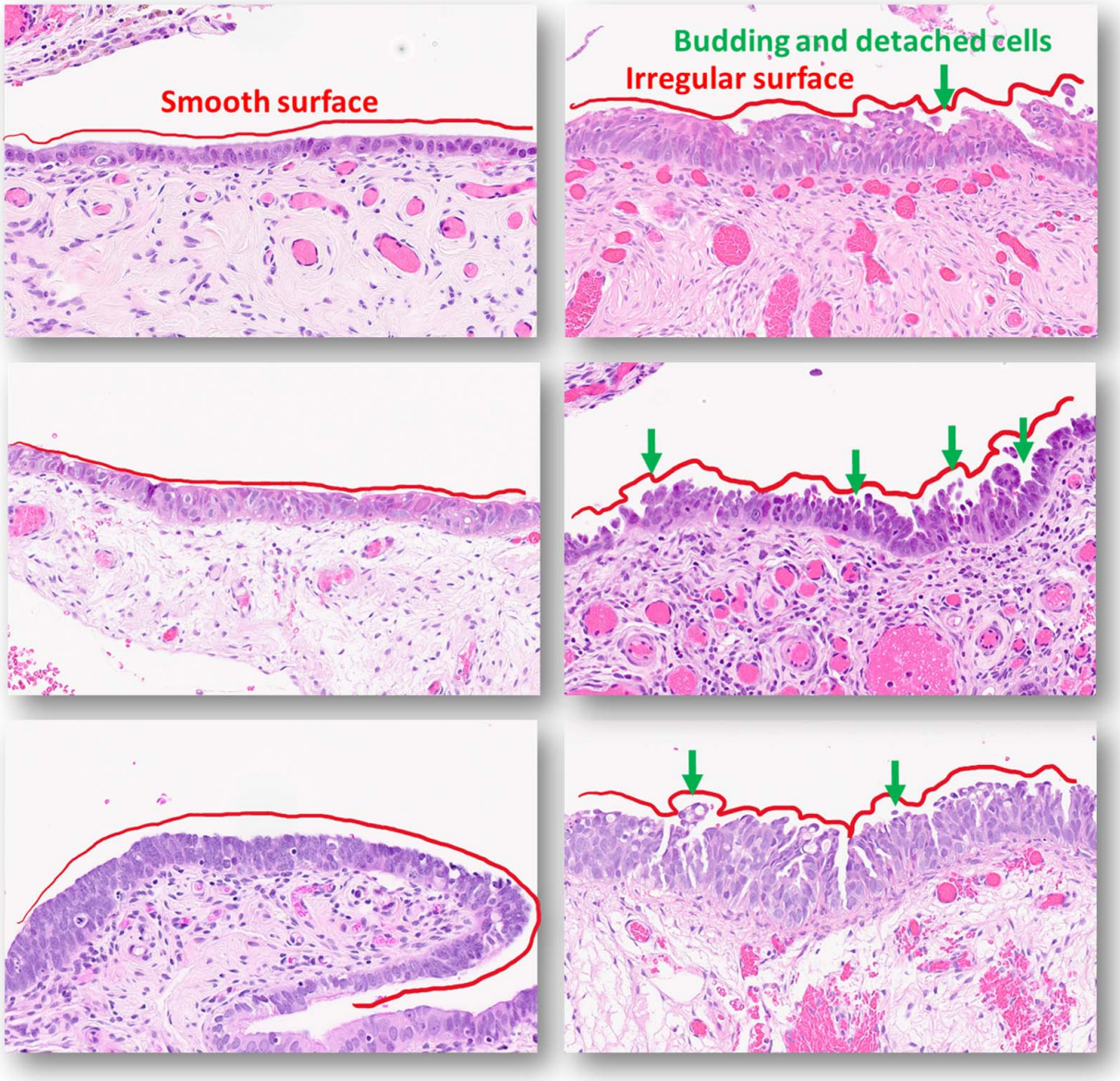

FIGURE 3. Representative STICs with BLAD and Flat features. Flat lesions with smooth and intact surface outlined by red lines (left column); BLAD lesions with irregular surface outlined by red lines featuring budding or detached cells marked by green arrows (right column).

on comparing the occurrence of BLAD and Flat lesions in Path 2 and Path 3. Our data showed that 25 of 36 (69%) BLAD lesions and 10 of 38 (26%) Flat lesions had Path 2 aneuploidy pattern, while 9 of 36 (25%) BLAD lesions and 11 of 38 (29%) Flat lesions had Path 3 aneuploidy pattern. Therefore, the Path 2 aneuploidy pattern, characterized by *CCNE1* gain/amplification, was associated with BLAD morphology ($P = 0.0004$) (Fig. 6B, left). Subset analysis of incidental tubal precursor lesions showed that 6 of 10 (60%) BLAD lesions and 3 of 22 (14%) Flat lesions had Path 2 aneuploidy pattern. Thus, the association between BLAD morphology and Path 2 aneuploidy pattern (*CCNE1* gain/amplification) remained significant for lesions in the incidental subgroup ($P = 0.013$) (Fig. 6B, right).

Multivariate Analysis of Ki-67 Proliferation Index

Since proliferative activity is one of the most prominent features of neoplasia, we examined which factor(s) were independently associated with an elevated Ki-67 labeling index. Multivariate analysis showed BLAD morphology and STIC diagnosis to be independently associated with increased Ki-67 proliferation index. As mentioned in the previous section, the Ki-67 proliferation index was 3.3 times higher (21.3% ± 20.1%) in BLAD

Copyright © 2024 The Author(s). Published by Wolters Kluwer Health, Inc.

Downloaded from http://journals.lww.com/ajsp by BhDMf5ePHKav1zEoum1tQfN4a+kJLhEZgbsIHo4XMi0hCywCX1AWnYQp/IlQrHD3i3D0OdRyi7TvSFl4Cf3VC4/OAVpDDa8K2+Ya6H515kE= on 09/11/2024

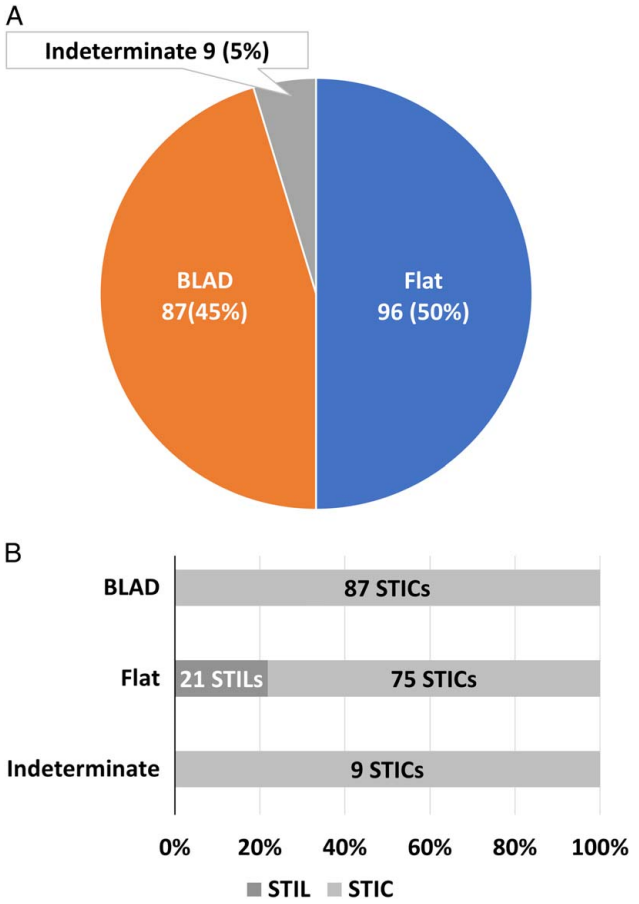

FIGURE 4. Results of classification of BLAD versus Flat morphological patterns. (A) Numbers and percentages of BLAD, Flat, and indeterminate lesions; (B) Bar graph shows diagnosis of the lesions in each group by percentage.

lesions than that in Flat lesions (6.5% ± 8.7%). After adjusting for STIC diagnosis, the BLAD morphology remained to be independently associated with an elevated Ki-67 labeling index ($P < 0.0001$), while the presence of multilayered epithelial stratification showed a marginally positive association with increased Ki-67 proliferation index ($P = 0.0695$). For incidental tubal precursor lesions (no concurrent HGSC), the Ki-67 proliferation index was 5.5 times higher in incidental BLAD lesions (24.1% ± 19.5%) than in incidental Flat lesions (4.4% ± 4.5%). Furthermore, Ki-67 proliferation index in incidental lesions with multilayered epithelial stratification (15.1% ± 16.8%) than in incidental lesions with a single layer of epithelium (3.5% ± 4.5%). In multivariate analysis, both BLAD morphology and multilayered epithelial stratification were independently associated with an elevated Ki-67 index ($P = 0.0036$), even after adjusting for STIC diagnosis ($P = 0.0023$).

Further analysis showed that lesions which had both BLAD morphology and the Path 2 aneuploidy pattern had higher Ki-67 proliferation indexes than the rest ($P < 0.0001$) (Fig. 7A, left). A similar finding was also observed in the incidental subgroup of lesions without concurrent HGSC ($P = 0.0047$) (Fig. 7A, right). Photomicrographs from representative cases are shown in Figure 7B. To determine the combination of morphologic features that best predict the proliferative activity in tubal lesions, we developed the following 3 groups as shown in Figure 7C: group 1 included any lesion exhibiting BLAD morphology; group 2 included Flat and multilayered STIC lesions; group 3 contained all remaining lesions. Notably, these 3 groups exhibited markedly distinct Ki-67 proliferation indices, as determined by analysis of variance of $\log_2$-transformed Ki-67 labeling indexes ($P < 0.0001$). In pair-wise comparisons, group 1 versus group 3 and group 2 versus group 3 significantly differed in normalized Ki-67 proliferation index ($P < 0.0001$). Normalized Ki-67 also significantly differed between group 1 and group 2 ($P = 0.023$).

DISCUSSION

Tubal precursor lesions preceding ovarian HGSC have been studied over the past 2 decades. Risk reduction salpingo-oophorectomy for high-risk women and opportunistic salpingectomy for average-risk women have been increasingly recommended because of their efficacy in reducing the incidence of HGSC. The safety and efficacy of a 2-step frimbriectomy followed by oophorectomy have been supported by a recent study with a median follow-up of 7.3 years.[30] Given the adoption of salpingectomy as a primary prevention strategy for HGSC, pathologists expect to encounter an increasing number of tubal precursor lesions incidentally diagnosed without concurrent HGSC. Since a significant number of women diagnosed with STICs experience recurrence as a disseminated HGSC after a 10-year follow-up,[9,23,24] better understanding of the malignant potential of tubal precursors is needed, which starts with more detailed characterization of their morphologic and molecular features.

Here, we focused on morphologic features, BLAD versus Flat, as the foundation to explore the risk stratification of incidental STICs and STILs. Although STICs showing a discohesive growth pattern have been briefly mentioned in a previous report[16] and has been used by some pathologists to assist in the diagnosis of an STIC, this is the first study to investigate these 2 morphologic subtypes of tubal precursor lesions. We carefully analyzed morphologic heterogeneity in the largest cohort of STIC and STIL lesions known so far for pathologic, molecular, and clinical correlation.

The major finding in this study is the recognition of the BLAD morphologic pattern in STICs, which includes budding, loosely adherent, and detached tubal epithelial cells with nuclear atypia. These features were combined for the purpose of statistical analysis based on the assumption that they represent discohesive STIC cells. Our data suggest that tubal precursor lesions represent a histologically heterogeneous group. While the biological significance of STIC lesions with BLAD morphology can only be

Copyright © 2024 The Author(s). Published by Wolters Kluwer Health, Inc.

Downloaded from http://journals.lww.com/ajsp by BhDMf5ePHKav1zEoum1tQfN4a+kJLhEZgbsIHo4XMi0hCywCX1AWnYQp/IlQrHD3i3D0OdRyi7TvSFl4Cf3VC4/OAVpDDa8K2+Ya6H515kE= on 09/11/2024

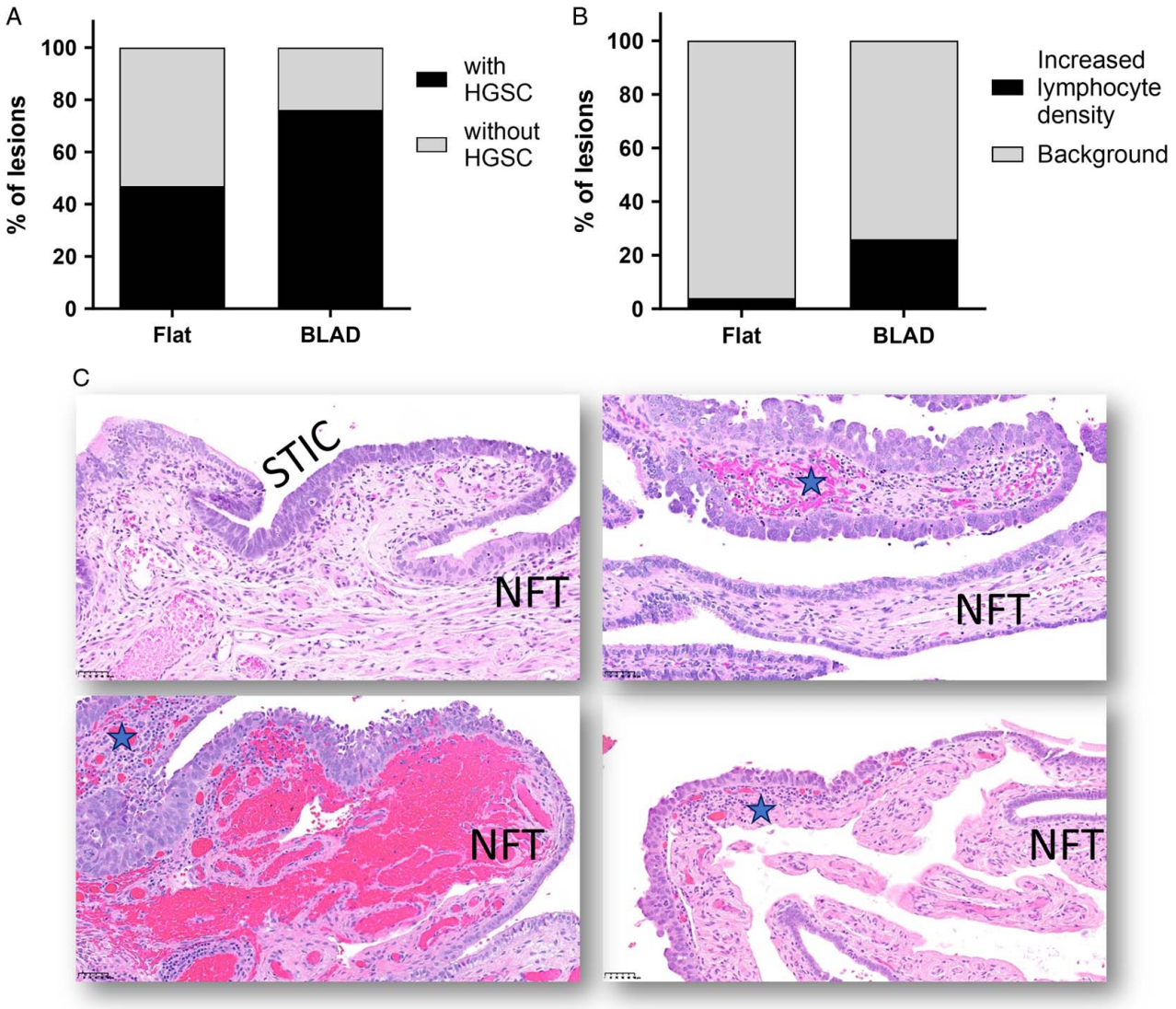

FIGURE 5. Clinicopathologic features in BLAD and Flat lesions. (A) A bar graph showing percentage of BLAD lesions with concurrent HGSC at the time of diagnosis of tubal precursor lesions; (B) A bar graph showing percentage of BLAD lesions with increased lymphocytic infiltrate compared with Flat lesions; (C) Representative lesions with increased lymphocytes (marked by star) compared with adjacent NFT tissue. NFT indicates normal-appearing fallopian tube.

surmised, several possibilities can be considered. Cells from morphologically BLAD STICs could be more easily exfoliated or dislodged from the lesion surface and spread to adjacent organs and soft tissues such as ovary, omentum, mesentery, and peritoneal surface, ultimately resulting in HGSC dissemination. At the same time, BLAD STIC cells may be more likely than Flat STIC cells to drop from the fallopian tube into the uterine cavity and arrive at the cervix, where routine liquid-based cytologic sampling akin to Papanicolaou test can detect their presence through molecular genetic assays. It has been reported that such strategies using DNA-based markers are able to detect early-stage ovarian cancer.[31]

Morphologically, BLAD STICs have an increased Ki-67 proliferation index and specific aneuploidy patterns, including *CCNE1* copy number gain, a molecular genetic feature characterizing many HGSCs.[32,33] Ki-67 proliferation index is considered to represent the degree of proliferative activity and in the current study a normalized Ki-67 index was also used on account of variability in baseline proliferative status. *CCNE1* gain/amplification has been validated by fluorescence in situ hybridization in 22% of STICs,[19] a result similar to the data from this study using RealSeqS. It has been reported that *CCNE1* gain/amplification also occurs in the precursor lesions of uterine serous carcinoma,[34] and the activated cyclin E1 pathway participates in tumor initiation and progression in a variety of human malignancies through promoting cell cycle advancement, tumor cell motility, and invasion.[35] The increased Ki-67 proliferation index and *CCNE1* copy

Copyright © 2024 The Author(s). Published by Wolters Kluwer Health, Inc.

Downloaded from http://journals.lww.com/ajsp by BhDMf5ePHKav1zEoum1tQfN4a+kJLhEZgbsIHo4XMi0hCywCX1AWnYQp/IlQrHD3i3D0OdRyi7TvSFl4Cf3VC4/OAVpDDa8K2+Ya6H515kE= on 09/11/2024

TABLE 1. The Relevant Clinicopathologic and Molecular Features in This Cohort

	All lesions			Lesions without concurrent HGSC		
Markers	**Flat n = 96**	**BLAD n = 87**	***P****	**Flat n = 51**	**BLAD n = 21**	***P****
Presence of a concurrent HGSC						
No	51	21	< 0.0001	—	—	—
Yes	45	66	—	—	—	—
STIC or STIL diagnosis						
STIL	21	0	< 0.0001	20	0	0.0003
STIC	75	87	—	31	21	—
Lesion layering						
Single layer	55	9	< 0.0001	26	1	< 0.0001
Multilayer	38	75	—	22	20	—
Indeterminate	3	3	—	3	0	—
Lymphocyte						
Increased	4	22	< 0.0001	1	5	0.0058
Not increased	92	62	—	50	15	—
Indeterminate	0	3	—	0	1	—
Ki-67 (normalized)	6.5 ± 8.7	21.3 ± 20.1	< 0.0001	4.4 ± 4.5	24.6 ± 19.1	< 0.0001
Aneuploidy						
2	10	25	< 0.0001	3	6	0.0063
3	11	9	—	6	4	—
4	14	2	—	10	0	—
5	3	0	—	3	0	—
N/A	58	51	—	29	11	—
Aneuploidy (path 2 vs. others)						
2	6	20	0.0004	3	6	0.0126
3, 4, 5	23	9	—	19	4	—

*Fisher exact test for categorical variables, and Wilcoxon rank-sum test for continuous variables. Significance, $P < 0.05$.

number of morphologically BLAD STICs raises the possibility that the BLAD morphologic pattern may increase the fitness of tumor cells once they are relocated to the peritoneal cavity and increase the risk of later development of HGSC when STICs are found at the time of salpingectomy. Since the follow-up of women with incidental STICs is either not long enough or not accessible, especially in consultation cases, we were not able to compare clinical outcomes associated with BLAD versus Flat tubal precursor lesions, but this will be a future goal.

We observed that BLAD morphology was more commonly seen in specimens with concurrent HGSC. One of the explanations is that BLAD lesions may represent superficial spread of the HGSC rather than the bona fide precursor lesions. If the latter were the case, it would be challenging to depict a scenario under which the original precursor lesion remained extant after HGSC emerges because the bulk of tumor would likely destroy or replace the minute in situ lesion. Indeed, next-generation sequencing has suggested that some of the presumed "STICs" are metastasis derived from HGSCs rather than true precursor lesions.[36] Therefore, we believe that the most appropriate approach to comparing BLAD and Flat lesions is to analyze incidental lesions (no concurrent HGSC) to exclude this confounding factor. By separating incidental lesions from the entire cohort, we found that the incidental BLAD lesions also have an elevated Ki-67 proliferation index, *CCNE1* amplification, and an increased stromal lymphocytic infiltrate.

An increased lymphocyte infiltration in some BLAD lesions is of great interest. To the best of our knowledge, this finding is the first analysis of the immune microenvironment in ovarian cancer precursor lesions. Human fallopian tubes contain a highly heterogeneous immune cell population including $CD163^+$ macrophages, $CD11c^+$ dendritic cells, and $CD8^+$ T cells, as well as several minor populations of $CD56^+$ NK cells, $CD4^+$ T cells, $CD20^+$ B cells, TCRγδ+ T cells, and $CD207^+$ Langerhans cells.[37] Given the roles of the tumor immune microenvironment in the development of malignancy and in determining the efficacy of immunotherapy against tumors, our findings point us in an important research direction to further identify the changes in the immune landscape in STICs as compared with normal-appearing fallopian tubes using multiplex immunostaining or single cell spatial studies.

Since there are several features distinguishing BLAD from Flat morphology as described herein, it is essential to

TABLE 2. Grouping the Tubal Precursor Lesions by the Combination of Normalized Ki-67 Index (Ratio of Index in a Lesion/Normal Fallopian Tube Epithelium) and Layering Feature

Group	Definition	BLAD lesions	Flat lesions	Total
1	Normalized Ki-67 < 5.67	16	62	78
2	Normalized Ki-67 ≥ 5.67 and single layer	7	12	19
3	Normalized Ki-67 ≥ 5.67 and multilayer	55	11	66

Fisher exact test shows that group is significantly associated with BLAD ($P < 0.0001$).

Copyright © 2024 The Author(s). Published by Wolters Kluwer Health, Inc.

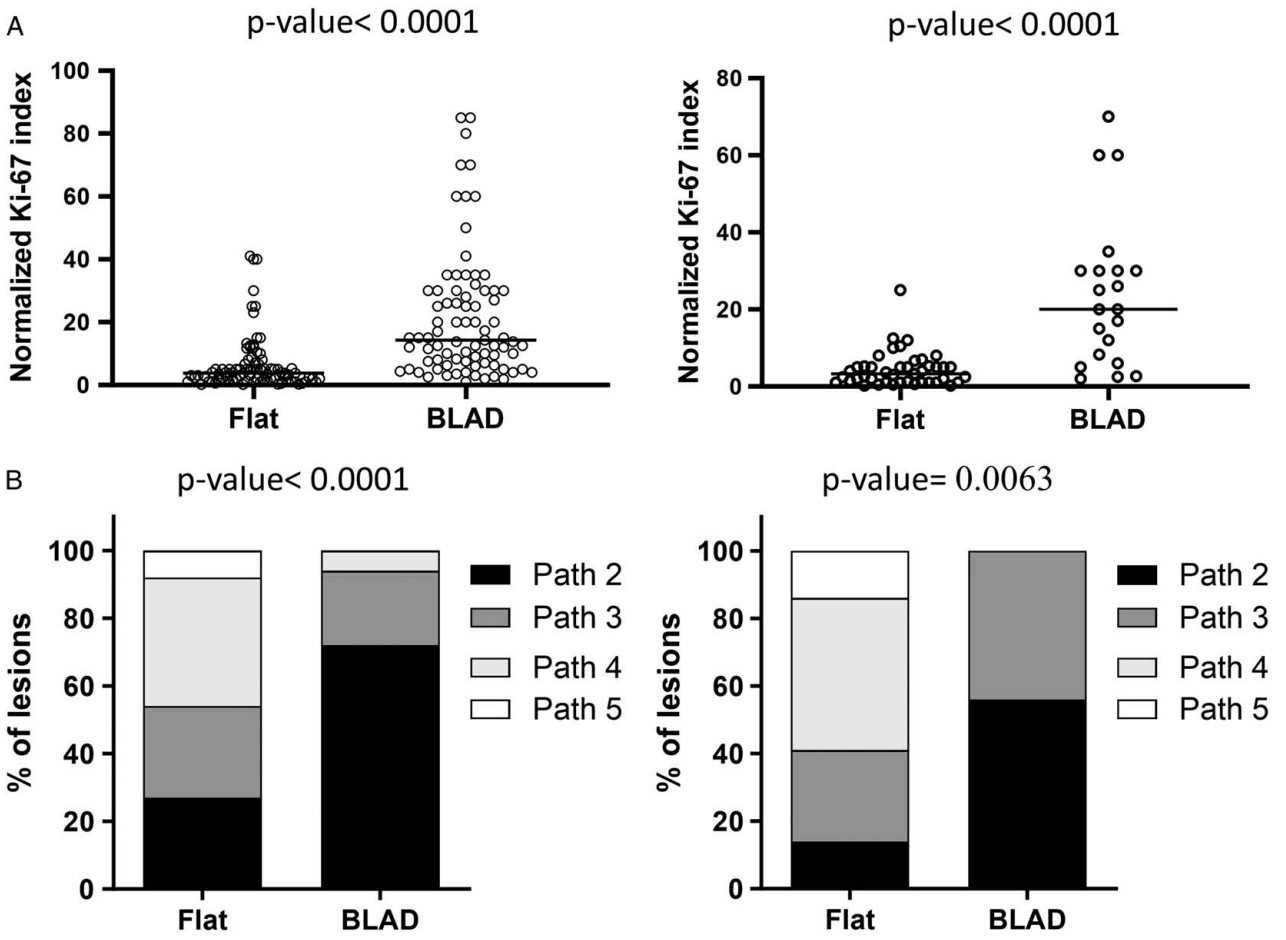

FIGURE 6. Comparisons of proliferative activities between BLAD lesions and Flat lesions in the entire cohort (left) and within the subgroup without concurrent HGSC (right). A, Scatter plots showing proliferative status, represented by normalized Ki-67 proliferation index, in BLAD lesions and Flat lesions. B, Percentage in bar graphs showing the distribution of specific aneuploidy patterns in BLAD lesions and in Flat lesions. The BLAD lesions are exclusively associated with the Path 2 aneuploidy pattern characterized by *CCNE1* amplification.

delineate which factors are independently associated with these morphologic subtypes. The multivariate analysis shows that Ki-67, multilayered epithelial stratification, and increased lymphocyte density are independently associated with the BLAD morphologic pattern. Furthermore, BLAD morphology was strongly associated with the combination of Ki-67 expression and multilayered epithelial stratification. It is possible that the development of a precursor lesion into a BLAD pattern rather than a Flat pattern depends on increased cellular proliferation, which promotes stratification of the lesion cells into a multilayered structure. However, the proliferative activity itself may not be sufficient to account for BLAD morphology since several Flat lesions also showed an increase in Ki-67 labeling index. The association between BLAD morphology and Path 2 aneuploidy pattern suggests *CCNE1* copy number gain/amplification may play a role.[19,33]

There are several limitations to this study beyond the lack of long-term follow-up in our cohort. Although the morphologic distinction between BLAD and Flat lesions appears to be straightforward, we noted that 5% of the precursor lesions fell into the indeterminate category. In the future, it is important to further refine lesional subtyping using improved morphologic criteria in combination with other factors. Artificial intelligence-assisted efforts can also be helpful. Moreover, we do not have multiomics data from this cohort of specimens. From this perspective, a future ovarian precancer atlas, using a format like the NCI Human Tumor Atlas Network, is needed to better understand the pathogenesis of STICs and catalog clinically aggressive types of STICs. This would be helpful for contextualizing morphologically BLAD lesions in the precursor landscape of the fallopian tube epithelium. It is also critical to determine whether increased cyclin E1 expression and activity contribute to the BLAD phenotypes using fallopian tube organoid models.

In conclusion, we report 2 distinct morphologic patterns of tubal precursor lesions with substantial agreement among pathologists. The tubal lesions with BLAD morphology represent ~45% of all the lesions.

Downloaded from http://journals.lww.com/ajsp by BhDMf5ePHKav1zEoum1tQfN4a+kJLhEZgbsIHo4XMi0hCywCX1AWnYQp/IlQrHD3i3D0OdRyi7TvSFl4Cf3VC4/OAVpDDa8K2+Ya6H515kE= on 09/11/2024

Copyright © 2024 The Author(s). Published by Wolters Kluwer Health, Inc.

Downloaded from http://journals.lww.com/ajsp by BhDMf5ePHKav1zEoum1tQfN4a+kJLhEZgbsIHo4XMi0hCywCX1AWnYQp/IlQrHD3i3D0OdRyi7TvSFl4Cf3VC4/OAVpDDa8K2+Ya6H515kE= on 09/11/2024

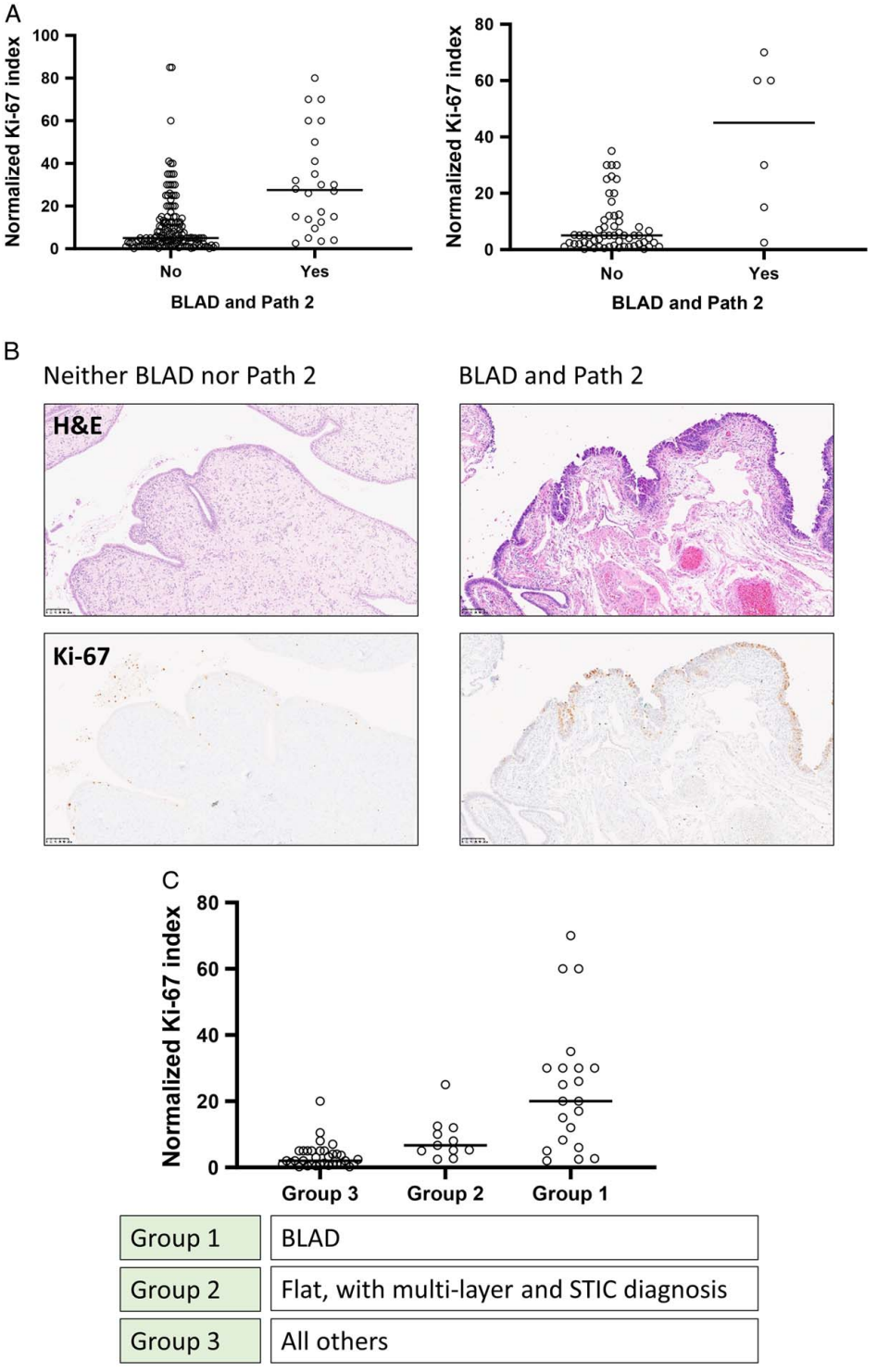

FIGURE 7. Multivariate analysis in predicting proliferative activity. A, Scatter plots showing synergy by combining BLAD pattern and Path 2 aneuploidy pattern to best predict elevation of Ki-67 index both in the complete cohort analysis (left) and in the subgroup lesions without concurrent HGSC (right). B, Representative lesions of each group with H&E staining (upper row) and with Ki-67 staining (lower row). C, Scatter plot depicting prediction of elevated Ki-67 index in 3 groups of tubal precursor lesions defined by the combination of BLAD versus Flat pattern, layering feature, and STIC diagnosis. H&E indicates hematoxylin and eosin staining.

Copyright © 2024 The Author(s). Published by Wolters Kluwer Health, Inc.

Downloaded from http://journals.lww.com/ajsp by BhDMf5ePHKav1zEoum1tQfN4a+kJLhEZgbsIHo4XMi0hCywCX1AWnYQp/IlQrHD3i3D0OdRyi7TvSFl4Cf3VC4/OAVpDDa8K2+Ya6H515kE= on 09/11/2024

They are associated with a higher proliferative activity, increased lymphocytic infiltrate, concurrent HGSC, and a specific aneuploidy pattern involving *CCNE1* amplification. The morphologic patterns can be used as a basis for clinical correlative studies aimed at risk stratifying of tubal precursor lesions and analysis of the molecular underpinnings in the development of HGSC.

REFERENCES

1. Shih IM, Wang Y, Wang TL. The origin of ovarian cancer species and precancerous landscape. *Am J Pathol*. 2021;191:26–39.
2. Piek JM, van Diest PJ, Zweemer RP, et al. Dysplastic changes in prophylactically removed Fallopian tubes of women predisposed to developing ovarian cancer. *J Pathol*. 2001;195:451–456.
3. Crum CP, Drapkin R, Miron A, et al. The distal fallopian tube: a new model for pelvic serous carcinogenesis. *Curr Opin Obstet Gynecol*. 2007;19:3–9.
4. Labidi-Galy SI, Papp E, Hallberg D, et al. High grade serous ovarian carcinomas originate in the fallopian tube. *Nat Commun*. 2017;8:1093.
5. Wu RC, Wang P, Lin SF, et al. Genomic landscape and evolutionary trajectories of ovarian cancer precursor lesions. *J Pathol*. 2019;248:41–50.
6. Eckert MA, Pan S, Hernandez KM, et al. Genomics of ovarian cancer progression reveals diverse metastatic trajectories including intraepithelial metastasis to the fallopian tube. *Cancer Dis*. 2016;6:1342–1351.
7. Crum CP, McKeon FD, Xian W. BRCA, the oviduct, and the space and time continuum of pelvic serous carcinogenesis. *Int J Gynecol Cancer*. 2012;22(suppl 1):S29–S34.
8. Kuhn E, Kurman RJ, Vang R, et al. TP53 mutations in serous tubal intraepithelial carcinoma and concurrent pelvic high-grade serous carcinoma- evidence supporting the clonal relationship of the two lesions. *J Pathol*. 2012;226:421–426.
9. Ruel-Laliberte J, Kasasni SM, Oprea D, et al. Outcome and management of serous tubal intraepithelial carcinoma following opportunistic salpingectomy: systematic review and meta-analysis. *J Obstet Gynaecol Can*. 2022;44:1174–1180.
10. Vang R, Visvanathan K, Gross A, et al. Validation of an algorithm for the diagnosis of serous tubal intraepithelial carcinoma. *Int J Gyn Pathol*. 2012;31:243–253.
11. Bogaerts JMA, van Bommel MHD, Hermens R, et al. Consensus based recommendations for the diagnosis of serous tubal intra-epithelial carcinoma: an international Delphi study. *Histopathology*. 2023;83:67–79.
12. Bogaerts JMA, Steenbeek MP, van Bommel MHD, et al. Recommendations for diagnosing STIC: a systematic review and meta-analysis. *Virchows Arch*. 2022;480:725–737.
13. Wang Y, Huang P, Wang BG, et al. Spatial transcriptomic analysis of ovarian cancer precursors reveals reactivation of IGFBP2 during pathogenesis. *Cancer Res*. 2022;82:4528–4541.
14. Kuhn E, Kurman RJ, Sehdev AS, et al. Ki-67 labeling index as an adjunct in the diagnosis of serous tubal intraepithelial carcinoma. *Int J Gynecol Pathol*. 2012;31:416–422.
15. Crum CP, Davidson B, Konishi I, et al. Tumours of the fallopian tube: High-grade serous carcinomaBoard. WCoTE. *Female Genital Tumours WHO Classification of Tumours*, 5th Edition. International Agency for Research on Cancer; 2020:219–220.
16. Meserve EEK, Brouwer J, Crum CP. Serous tubal intraepithelial neoplasia: the concept and its application. *Mod Pathol*. 2017;30:710–721.
17. Vang R, Shih IM. Serous tubal intra-epithelial carcinoma: what do we really know at this point? *Histopathology*. 2022;81:542–555.
18. Asaka S, Davis C, Lin SF, et al. Analysis of telomere lengths in p53 signatures and incidental serous tubal intraepithelial carcinomas without concurrent ovarian cancer. *Am J Surg Pathol*. 2019;43:1083–1091.
19. Kuhn E, Wang TL, Doberstein K, et al. CCNE1 amplification and centrosome number abnormality in serous tubal intraepithelial carcinoma: further evidence supporting its role as a precursor of ovarian high-grade serous carcinoma. *Mod Pathol*. 2016;29:1254–1261.
20. Pisanic TR II, Wang Y, Sun H, et al. Methylomic landscapes of ovarian cancer precursor lesions. *Clin Cancer Res*. 2020;26:6310–6320.
21. Stone R, Sakran JV, Long Roche K. Salpingectomy in ovarian cancer prevention. *JAMA*. 2023;329:2015–2016.
22. Wagar MK, Forlines GL, Moellman N, et al. Postpartum opportunistic salpingectomy compared with bilateral tubal ligation after vaginal delivery for ovarian cancer risk reduction: a cost-effectiveness analysis. *Obstet Gynecol*. 2023;141:819–827.
23. Steenbeek MP, van Bommel MHD, Bulten J, et al. Risk of peritoneal carcinomatosis after risk-reducing salpingo-oophorectomy: a systematic review and individual patient data meta-analysis. *J Clin Oncol*. 2022;40:1879–1891.
24. Linz VC, Lowe A, van der Ven J, et al. Incidence of pelvic high-grade serous carcinoma after isolated STIC diagnosis: a systematic review of the literature. *Front Oncol*. 2022;12:951292.
25. Li L, Antero MF, Zhang M, et al. Mutation and methylation profiles of ectopic and eutopic endometrial tissues. *J Pathol*. 2021;255:387–398.
26. Yemelyanova A, Vang R, Kshirsagar M, et al. Immunohistochemical staining patterns of p53 can serve as a surrogate marker for TP53 mutations in ovarian carcinoma: an immunohistochemical and nucleotide sequencing analysis. *Mod Pathol*. 2011;24:1248–1253.
27. Douville C, Cohen JD, Ptak J, et al. Assessing aneuploidy with repetitive element sequencing. *Proc Natl Acad Sci USA*. 2020;117:4858–4863.
28. Douville C, Moinova HR, Thota PN, et al. Massively parallel sequencing of esophageal brushings enables an aneuploidy-based classification of patients with Barrett's esophagus. *Gastroenterology*. 2021;160:2043–2054 e2042.
29. Wang Y, Douville C, Chien YW, et al Aneuploidy landscape in precursors of ovarian cancer. *Clin Cancer Res*. 2024;30:600–615.
30. Leblanc E, Narducci F, Ferron G, et al. Prophylactic radical fimbriectomy with delayed oophorectomy in women with a high risk of developing an ovarian carcinoma: results of a prospective national pilot study. *Cancers (Basel)*. 2023;15:1141.
31. Wang Y, Li L, Douville C, et al. Evaluation of liquid from the Papanicolaou test and other liquid biopsies for the detection of endometrial and ovarian cancers. *Sci Transl Med*. 2018;10:eaap879.
32. Bell D, Berchuck A, Birrer M, et al. Integrated genomic analyses of ovarian carcinoma. *Nature*. 2011;474:609–615.
33. Nakayama K, Nakayama N, Jinawath N, et al. Amplicon profiles in ovarian serous carcinomas. *Int J Cancer*. 2007;120:2613–2617.
34. Kuhn E, Bahadirli-Talbott A, Shih Ie M. Frequent CCNE1 amplification in endometrial intraepithelial carcinoma and uterine serous carcinoma. *Mod Pathol*. 2014;27:1014–1019.
35. Nakayama K, Rahman MT, Rahman M, et al. CCNE1 amplification is associated with aggressive potential in endometrioid endometrial carcinomas. *Int J Oncol*. 2016;48:506–516.
36. McDaniel AS, Stall JN, Hovelson DH, et al. Next-generation sequencing of tubal intraepithelial carcinomas. *JAMA Oncol*. 2015;1:1128–1132.
37. Ardighieri L, Lonardi S, Moratto D, et al. Characterization of the immune cell repertoire in the normal fallopian tube. *Int J Gynecol Pathol*. 2014;33:581–591.

Copyright © 2024 The Author(s). Published by Wolters Kluwer Health, Inc.